AD-A136 331

TECHNICAL
LIBRARY

AD

TECHNICAL REPORT ARLCB-TR-83032

ELECTRICAL TRANSPORT IN LOW RESISTIVITY AMORPHOUS ALLOYS

L. V. MEISEL

P. J. COTE

SEPTEMBER 1983

US ARMY ARMAMENT RESEARCH AND DEVELOPMENT CENTER
LARGE CALIBER WEAPON SYSTEMS LABORATORY
BENÉT WEAPONS LABORATORY
WATERVLIET N.Y. 12189

APPROVED FOR PUBLIC RELEASE; DISTRIBUTION UNLIMITED

DISCLAIMER

The findings in this report are not to be construed as an official Department of the Army position unless so designated by other authorized documents.

The use of trade name(s) and/or manufacturer(s) in this report does not constitute an official indorsement or approval.

DISPOSITION

Destroy this report when it is no longer needed. Do not return it to the originator.

SECURITY CLASSIFICATION OF THIS PAGE *(When Dete Entered)*

REPORT DOCUMENTATION PAGE		READ INSTRUCTIONS BEFORE COMPLETING FORM
1. REPORT NUMBER ARLCB-TR-83032	2. GOVT ACCESSION NO.	3. RECIPIENT'S CATALOG NUMBER
4. TITLE *(and Subtitle)* ELECTRICAL TRANSPORT IN LOW RESISTIVITY AMORPHOUS ALLOYS		5. TYPE OF REPORT & PERIOD COVERED Final 6. PERFORMING ORG. REPORT NUMBER
7. AUTHOR(s) L. V. Meisel and P. J. Cote		8. CONTRACT OR GRANT NUMBER(s)
9. PERFORMING ORGANIZATION NAME AND ADDRESS US Army Armament Research & Development Center Benet Weapons Laboratory, DRSMC-LCB-TL Watervliet, NY 12189		10. PROGRAM ELEMENT, PROJECT, TASK AREA & WORK UNIT NUMBERS AMCMS NO.6111.02.H600.011 PRON NO.1A325B541A1A
11. CONTROLLING OFFICE NAME AND ADDRESS US Army Armament Research & Development Center Large Caliber Weapon Systems Laboratory Dover, NJ 07801		12. REPORT DATE Sept. 1983 13. NUMBER OF PAGES 33
14. MONITORING AGENCY NAME & ADDRESS*(if different from Controlling Office)*		15. SECURITY CLASS. *(of this report)* Unclassified 15a. DECLASSIFICATION/DOWNGRADING SCHEDULE

16. DISTRIBUTION STATEMENT *(of this Report)*

Approved for Public Release,Distribution Ullimited

17. DISTRIBUTION STATEMENT *(of the ebstract entered in Block 20, if different from Report)*

18. SUPPLEMENTARY NOTES Presented at the meeting of American Physical Society, March 1983. Submitted to the Journal, Physical Review.

19. KEY WORDS *(Continue on reverse side if necessary and identify by block number)*

Electrical Transport
Amorphous Alloys
Diffraction Model
Saturation Effects

20. ABSTRACT *(Continue on reverse side if necessary and identify by block number)*

Diffraction model calculations incorporating appropriate scattering matrix elements and phonon ineffectiveness effects (saturation effects) yield results which are consistent with the observed temperature dependence of the electrical resistivity in low resistivity ($\rho < 100\ \mu\Omega cm$) amorphous alloys. In particular, remarkably good quantitative agreement with available detailed resistivity measurements in a-MgZn alloys has been obtained by these methods. The results
(CONT'D ON REVERSE)

DD FORM 1 JAN 73 1473 EDITION OF 1 NOV 65 IS OBSOLETE

SECURITY CLASSIFICATION OF THIS PAGE *(When Dete Entered)*

20. ABSTRACT (CONT'D)

further indicate that saturation effects, which dominate the temperature dependence of the high resistivity amorphous metals, are important even for resistivities as low as 50 μΩcm.

TABLE OF CONTENTS

TABLES

Page

LIST OF ILLUSTRATIONS

ACKNOWLEDGEMENTS

We thank Dr. U. Mizutani and Dr. T. Matsuda for their helpful comments and for providing data on a-MgZn prior to publication. We are also pleased to acknowledge the assistance of Ellen Fogarty in preparing the manuscript.

INTRODUCTION

Most quantitative theoretical results on electrical transport in amorphous metals have been obtained using the diffraction model[1-6] and its extensions[6-11] in which the electron-phonon interaction matrix element is assumed to be independent of the electron mean free path. We shall refer to such calculations in this report as applications of the standard diffraction model. The standard diffraction model also serves as the basis for the analysis of transport in crystalline metals, yielding Bloch-Gruneisen theory[12] for normal scattering processes. However, the standard diffraction model is of questionable validity for most amorphous metals whose resistivities are of the order of or greater than 150 μΩcm, which corresponds to electron mean free paths of the order of ionic spacings. The deviations of experimental results from the predictions of the standard diffraction model in high resistivity metals are referred to as "saturation effects" or Mooij phenomena.[6,13-17] In spite of the presence of saturation effects, the standard diffraction model gives reasonable values for the magnitude of the electrical resistivity and its concentration dependence in a number of amorphous alloys;[6,18] in fact, the model is often not observed to fail unless close attention is paid to details of the temperature dependence of the resistivity. We refer to treatments of electrical transport in which the electron-phonon interaction is electron mean free path dependent[16,17] as "saturated cases" of the diffraction model.

References are listed at the end of this report.

The treatment of Mooij phenomena has been the subject of considerable theoretical study. Some investigators have treated high resistivity metals in the context of the diffraction model by postulating interband tunneling channels[19] or, in analogy with the Pippard theory of ultrasonic attenuation in metals,[20] an electron mean free path dependent electron-phonon interaction.[16,17] Other investigators[21] have approached the problem by extending theories intended for transport in materials whose electrons are localized.

The standard diffraction model is expected to be valid when the electron mean free path is not too short. Thus, a test of the theory in low resistivity ($\rho < 100$ $\mu\Omega$cm) metallic glasses is of interest. Until recently, relatively few experiments have been performed on such alloys since they are difficult to fabricate. Notable exceptions were the results in vapor deposited a-CuSn[22] and a-AuSn[23] alloys for a wide range of compositions. These alloys exhibit the features predicted by the diffraction model including trends in ρ and the temperature coefficient of resistivity (TCR) with composition, and the presence of a maximum in ρ vs. T in alloys with a negative room temperature TCR, an essential feature of standard diffraction model predictions.[6]

There are now substantial data for low resistivity amorphous alloys. Matsuda and Mizutani completed a thorough study of electrical transport in a-MgZn alloys[24] from 2 to 300K with Zn concentrations ranging from 22.5 to 35 percent and in an a-MgCu alloy.[25] Mizutani and Yoshida[26] provided data on a variety of Ag-Cu based alloys from 77 to 300K. Earlier, Hafner et al[27] had found good agreement between experiment and the theory of References 7-9 in a preliminary study on a-Mg_7Zn_3. These alloys are particularly suited for tests

of the diffraction model because of their low resistivities (~ 50 μΩcm) and the existence of supporting data which determine the relevant parameters in the Ziman-Faber theory (e.g., Fermi wave number, k_F, and structure factor peak position, k_p). Moreover, the conduction electron states in a-MgZn may be assumed to be almost exclusively of s and p character in contrast to the complex situation in the more common transition-metal based glassy alloys.

In this report we compare the a-MgZn alloy transport data with results computed using the diffraction model with (i) Heine-Aberenkov pseudopotentials as tabulated by Harrison[28] used for the scattering matrix element in the Born approximation, and (ii) a phase shift expansion of the scattering matrix elements as developed by Evans et al.[29] Saturation effects are taken into account by invoking the Pippard-Ziman constraint on the electron-phonon interaction.[1,6,16,17] A brief review of the theory is given in the section below. The scattering potential is discussed in the section following the Theory, where the method of selecting phase shifts appropriate for a-MgZn is described; and the problems encountered with the Born approximation are discussed. In the section on Theoretical and Experimental Results, detailed comparison is made between the data on a-MgZn and the predicted results using the diffraction model with both the phase shift expansion and pseudopotential scattering matrix elements. Implications for transport in general low resistivity alloys are also described in that section. A summary and conclusions are given in the last section.

THEORY

The diffraction model (Ziman-Faber theory[5]) result for the electrical resistivity is

$$\rho = \frac{12\pi\Omega_o}{e^2 h V_F^2} \int_0^1 d\left(\frac{K}{2k_F}\right)\left(\frac{K}{2k_F}\right)^3 S\rho(K)\left|u(K)\right|^2 \qquad (1)$$

where Ω_o is the atomic volume, V_F the Fermi velocity, k_F the Fermi wave vector, K the scattering vector, h is Planck's constant divided by 2π, e is the electron charge, and the resistivity static structure factor $S\rho(K)$ is defined in terms of the Van Hove dynamical structure factor[4] $S(K,\omega)$ as

$$S\rho(K) = \int_{-\infty}^{\infty} d\omega x n(x) S(K,\omega) \qquad (2)$$

where $x = h\omega/k_B$, $n(x) = (e^x-1)^{-1}$, k_B is Boltzmann's constant, and T is the absolute temperature. The scattering matrix element u(K) is approximated by a pseudopotential in Born approximation or for strong scattering (i.e., large phase shifts), it can be expressed in terms of phase shifts[29] as

$$u(K) = \frac{2\pi h^3}{m(2mE_F)^{1/2}\Omega_o} \sum_{\ell}(2\ell+1)\sin\eta_\ell(E_F)e^{i\eta_\ell(E_F)}P_\ell(\cos\theta) \qquad (3)$$

where the phase shift $\eta_\ell(E_F)$ for angular momentum quantum number ℓ is evaluated at the Fermi energy and m is the electron mass. The matrix element in the form of Eq. (93) includes single site multiple scattering and is called the t-matrix. We shall discuss transport in a-MgZn alloys using both of these formulations. The general case is described in terms of the t-matrix.

The resistivity static structure factor in an amorphous Debye solid may be expanded in the form[6-9]

$$S\rho(K) = S_o\rho(K) + S_1\rho(K) + S_2\rho(K) + \ldots \qquad (4)$$

where $S_n^{\rho}(K)$ is an n-phonon term. The elastic scattering term (no phonons) is

$$S_o^{\rho}(K) = a(K)e^{-2W(K)} \tag{5}$$

where $e^{-2W(K)}$ is the Debye-Waller factor and the geometrical structure factor a(K) is

$$a(K) = \frac{1}{N} \sum_{m,n} \exp[i\bar{K}\cdot(\bar{m}-\bar{n})] \tag{6}$$

with m,n averaged ionic positions. The one phonon term, allowing for Pippard-Ziman phonon ineffectiveness as described in References 16 and 17, is

$$S_1^{\rho}(K) = \alpha(K)e^{-2W(K)} \frac{T}{\theta} \int_0^1 d\left(\frac{q}{q_D}\right) \left(\frac{q}{q_D}\right)^2 n(x)(n(x)+1) \int \frac{d\Omega q}{4\pi} a(|\bar{K}+\bar{q}|)F(q\Lambda) \tag{7}$$

where $\alpha(K) = 3(hK)^2/Mk_B\theta$ where M is the averaged ionic mass, q_D is the Debye wave number, Θ is the Debye temperature, $x = (\theta/T)(q/q_D)$ for a Debye solid, Λ is the electron mean free path, and $F(q\Lambda)$ describes the reduction in scattering effectiveness which occurs for small $q\Lambda$. The calculations presented here assume that $F(q\Lambda)$ can be represented by the form suggested by Pippard[20] in his study of ultrasonic attenuation, and

$$F(y) \equiv \frac{2}{\pi}\left[\frac{y\tan^{-1}y}{y-\tan^{-1}y} - \frac{3}{y}\right]. \quad \text{(Pippard saturation)} \tag{7a}$$

We refer to this expression as the Pippard function. If saturation effects can be ignored

$$F(y) = 1. \quad \text{(No saturation)} \tag{7b}$$

We refer to this form of the theory as the standard diffraction model. Equation (7b) is also clearly the long electron mean free path limit (or low resistivity limit) of the Pippard function. One can also represent saturation

effects with a "sharp cutoff" form

$$F(y) = \begin{matrix} 0 & y < y_c \\ 1 & y > y_c \end{matrix} \quad \text{(sharp cutoff)} \tag{7c}$$

where the cutoff value y_c is of order $q_D a$ where a is the mean ionic spacing. Note that the placement of $F(q\Lambda)$ in the one phonon part of the (generalized) resistivity static structure factor results from a decomposition of the absolute square of a phonon wave number and electron mean free path dependent electron-phonon matrix element into a simple product according to the prescription

$$|u(K,q\Lambda)|^2 = |u(K)|^2 F(q\Lambda)$$

where u(K) is the ordinary scattering matrix element which appears, for example, in the elastic scattering term.

The multiphonon series is approximated in various ways.[30] For the range of temperatures of interest here ($T \lesssim \theta$) the particular approximation made is not important and the results are given in Sham-Ziman approximation,[30] i.e., we assume that the effect of the multiphonon series is to cancel the Debye-Waller factor in the one-phonon term. We shall refer to that modified term as the inelastic scattering term or simply the phonon scattering term.

The Debye-Waller exponent is given (for Debye solid) by

$$2W(K) = \alpha(K) \int_0^1 d\left(\frac{q}{q_D}\right)\left(\frac{q}{q_D}\right)\left(n(x)+\frac{1}{2}\right) \tag{8a}$$

$$= \alpha(K)\left(\frac{T}{\theta}\right)^2 \int_0^{\theta/T} dx\, x\left(n(x)+\frac{1}{2}\right) \tag{8b}$$

Note that Eqs. (1) through (8) have been written in a form appropriate to a pure substance. The product $S^{\rho}(K)|u(K)|^2$ should be replaced by a sum of concentration dependent terms involving individual constituent scattering matrix elements and partial structure factors in alloy systems. Nevertheless, in the a-MgZn alloys we treat the material with a single effective scattering potential in the spirit of the substitutional model of Faber and Ziman[5] and a Percus-Yevick form[31] for the geometrical structure factor. This is not quite right when there is short range order and $2k_F$ is situated differently with respect to the peak positions of the various partial structure factors. However, a broad range of scattering vectors contribute to the resistivity in a-MgZn, the constituents have very similar atomic structure, and the computations by von Heimendal[32] suggest that the three partial structure factors are very similar; we thus assume that the conditions for the substitutional model obtain. The application of the substitutional model to the other low resistivity amorphous alloys considered here may not be as good an approximation.

THE SCATTERING MATRIX ELEMENT AND THE MAGNITUDE OF ρ

The atomic structure of Mg consists of filled shells and $3s^2$ electrons and similarly in Zn, filled shells, and $4s^2$ electrons. It follows from straightforward considerations of the atomic structure of these simple divalent metals that the appropriate starting structure in the metallic solid will consist of a nearly filled s band with some p band occupation resulting in a metallic sp band primarily of s-character with a small admixture of p-character. (Note that the energy required to promote an electron to a d-level in Mg or Zn is prohibitively large in constrast to the situation in

Ca, Sr, or Ba.) Thus, if we construct a scattering matrix element as given in Eq. (3), we expect the s-wave phase shift $\eta_0(E_F)$ to be slightly less than π, the p phase shift $\eta_1(E_F)$ to be small, and other phase shifts to be negligible. Such a scattering matrix element will be drastically different in form from a Born approximation pseudopotential matrix element. We have constructed such a matrix element for a-MgZn by adjusting $\eta_0(E_F)$ to give the observed magnitude of ρ with $\eta_1(E_F)$ constrained to satisfy the Friedel sum rule.[33] (Since there are only $\ell = 0$ and 1 phase shifts to consider and the electron per atom ratio, $z = 2$, one has to satisfy $\eta_0 + 3\eta_1 = \pi$.) The resulting values of $\eta_0(E_F)$ and $\eta_1(E_F)$ are 2.87 and 0.09 respectively; we use these values in our subsequent investigations of the temperature dependences.

Dunsworth[34] has deduced phase shifts for Zn in β brasses by adjusting APW-form matrix elements to fit experimentally determined Fermi surface features. His results for Zn in crystalline β brasses where $Z = 1.5$ electrons per atom are $\eta_o = 3.114$, $\eta_1 = 0.289$, and $\eta_2 = 0.001$ at the free electron Fermi energy. This lends support to our general expectation that the divalent metals and alloys will exhibit large $\ell = 0$ phase shifts (near π) and small $\ell = 1$ phase shifts.

It should be stressed that although the magnitude of ρ is quite sensitive to changes in the phase shifts, the T dependence of $\rho(T)/\rho(\theta)$ is relatively insensitive to specific phase shift values. For example, a matrix element constructed for $\eta_o = 2.00$ and $\eta_1 = 0.38$ yields a factor of two increase in ρ but only changes the temperature dependence of $\rho(T)/\rho(\theta)$ by about 5 percent over the range from 0°K to θ for the values of $2k_F/k_p$ studied here. In fact,

for $\frac{\pi}{2} \lesssim \eta_o \lesssim \pi$ and η_1 adjusted to satisfy the sum rule, the scattering matrix elements are similar in form to that shown in Figure 1 for $\eta_1 = 2.87$ and give essentially equivalent (i.e., within about 20 percent) temperature dependences for $\rho(T)/\rho(\theta)$.

Another point which should be considered is the effect on $\rho(T)$ of breakdown of the Freidel sum rule constraint. Although various forms of the Friedel sum rule[35,36] are invoked to constrain phase shifts evaluated at the Fermi energy, it should be noted that calculated phase shifts often fail to satisfy the sum rule; for example, in Reference 36 the phase shifts computed for Ca and Sr yield Friedel sums differing by 15 and 3 percent respectively from the sum rule. Again the form of the t-matrix, (which determines the temperature dependence of $\rho(T)/\rho(\theta)$) is preserved even for potentials which do not satisfy the sum rule as long as $\frac{\pi}{2} \lesssim \eta_o \lesssim \pi$ and η_1 is not too large.

The point of this discussion is that although the phase shifts deduced for a-MgZn are not uniquely determined by the transport data, the temperature dependence of the resistivity of all the low resistivity amorphous alloys studied to date can be discussed in terms of an approximate t-matrix of the form shown in Figure 1. Also one might expect the best phase shifts for a-MgZn to be given within about the deviations from the sum rule seen in Ca or Sr.

If one uses the Born approximation with Heine-Aberenkov pseudopotentials as tabulated in Reference 28 for Mg and Zn, approximates $S^{\rho}(K)$ by $S_o(K)$, and takes a value of k_F appropriate to the a-MgZn alloys, then one obtains 20 and 29 $\mu\Omega$cm respectively for the Mg and Zn pseudopotentials. The discrepancy

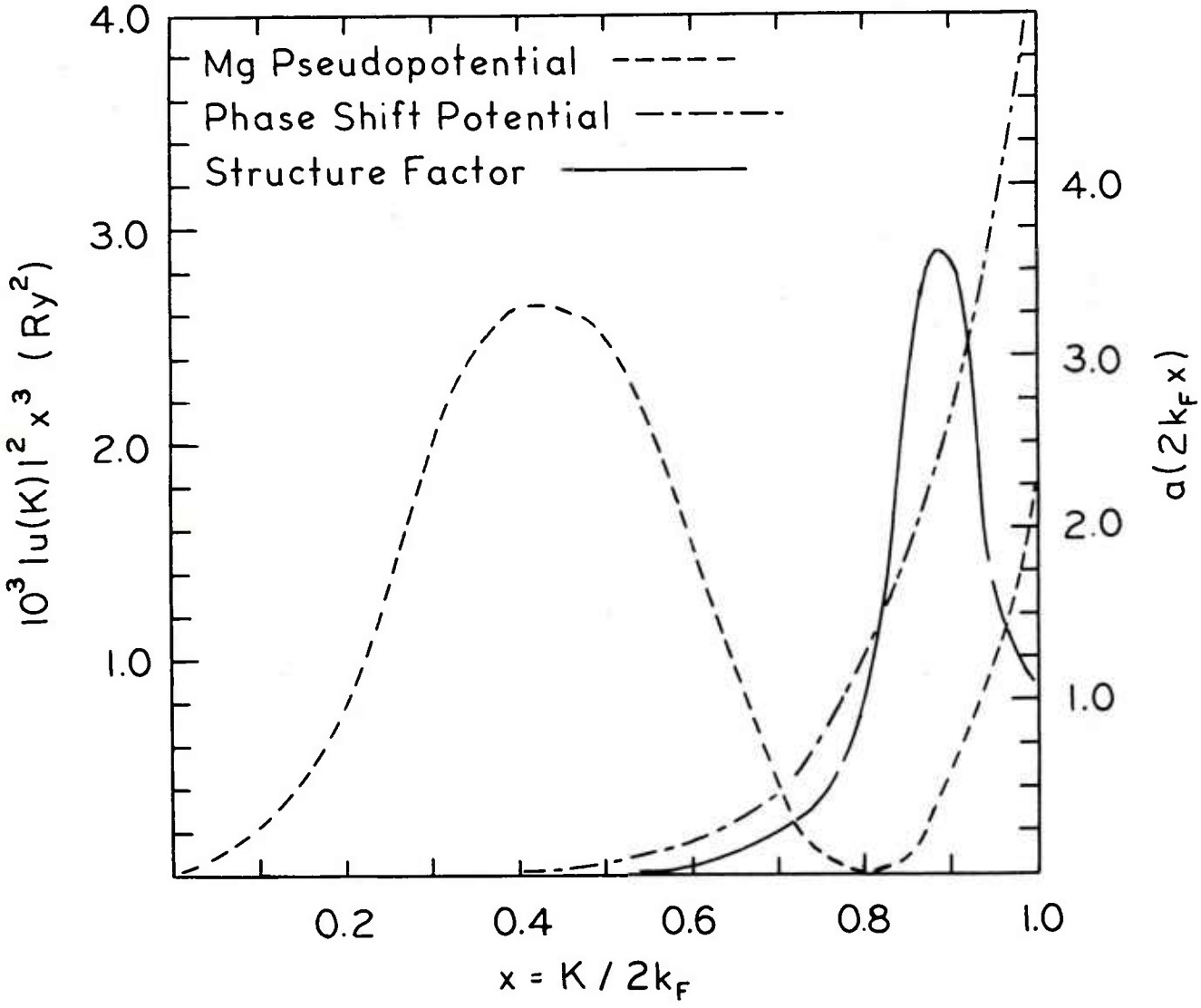

Figure 1. Weighted absolute squared potentials used to describe Transport in a-MgZn.

between either of these values and the measured resistivities of the a-MgZn alloys is of the order found when these methods have been applied to transport in liquid metals.[37] However, the form of the Born approximation matrix element is drastically different from that of the adjusted phase shift matrix element as may be seen in Figure 1. The cancellation near $2k_F$, which is characteristic of pseudopotentials, does not occur in the phase shift expanded matrix element.

Considering only the theoretical results for the magnitude of ρ, either approach can yield reasonable agreement with the data in a-MgZn alloys. However, we shall see in the section on Results that the phase shift matrix element leads to a better approximation to the observed temperature dependence in a-MgZn than the Born approximation results.

Moreover, there are well known examples of difficulties with Born approximation transport calculations in related systems. For example, the electrical resistivity computed with Heine-Aberenkov pseudopotentials in Born approximation and with Percus-Yevick hard sphere structure factors is in poor agreement with experiment in liquid Ca, Ba, and Sr. On the other hand, Ratti and Evans[38] obtained good agreement with the experimental data in liquid Ca, Ba, and Sr using a phase shift expanded form for the scattering matrix element (Eq. (3)) with phase shifts computed from muffin tin potentials. (The only significant phase shifts in these alkaline earth liquids were an s phase shift slightly less than π and a small d phase shift.)

Furthermore, there are even indications of difficulties with Born approximation for the treatment of transport in monovalent liquid metals. Young et al[36] concluded that Born approximation was inadequate in these liquid

metals and achieved improved agreement with electrical resistivity and thermopower in terms of phase shift expanded matrix elements (Eq. (3)). In the light of these findings for liquid Ca, Ba, and Sr and for the liquid monovalent metals, it is perhaps not surprising that we find that the temperature dependence of the electrical resistivity in a-MgZn and the other low resistivity amorphous alloys is better described by a scattering matrix element of the form of Eq. (3) (t-matrix) than by pseudopotentials in Born approximation.

COMPARISON OF THEORETICAL AND EXPERIMENTAL RESULTS

The parameters used in the computations are listed in Table I. They were based upon the following: x-ray and neutron diffraction[39] yield values of k_p in a-Mg_7Zn_3 of 2.7 and 2.6 $Å^{-1}$ respectively. Hall effect measurements by Matsuda and Mizutani[24] give 2.77 $Å^{-1} < 2k_F < 2.98$ $Å^{-1}$ for the range of compositions of a-MgZn studied. The mean ionic mass is used for M and in a-MgZn we take $q_D = k_F$ (since z = 2). Specific heat measurements[40] in a-Mg_7Zn_3 yield $\theta = 295K$. We have also assumed a Debye phonon spectrum and an effective (geometric) structure factor of Percus-Yevick form with packing fraction $\eta = 0.525$ (which is representative of structure factors found in amorphous alloys).

In the remainder of this report, when we refer to the saturated case, we are quoting results computed for Pippard saturation with $q_D\Lambda = 11.7$ in Eq. (7a), which produces a 25 percent reduction in the inelastic scattering part of the resistivity at $T = \theta$. (This is equivalent to assuming the saturation resistivity $\rho^* \approx 200$ $\mu\Omega$cm in the treatment of Reference 17.) We emphasize

here that inelastic scattering contributes less than five percent to the total ρ so that the effect of saturation in the adjusted phase shifts is negligible. The unsaturated case results are obtained from the standard diffraction model, i.e., using Eq. (7b) or letting $\Lambda \to \infty$ in Eq. (7a).

TABLE I. SUMMARY OF INPUT FOR RESISTIVITY CALCULATIONS IN a-MgZn. THE DEBYE TEMPERATURE θ WAS DETERMINED FROM SPECIFIC HEAT MEASUREMENTS,[40] THE POSITION OF THE FIRST PEAK IN THE STRUCTURE FACTOR k_p WAS DETERMINED BY NEUTRON DIFFRACTION,[39] AND THE FERMI WAVENUMBERS k_F WERE DEDUCED FROM HALL EFFECT MEASUREMENTS.[24] η IS THE HARD SPHERE PACKING FRACTION IN THE PERCUR-YEVICK FORMULA.[37]

Input	Descriptive	Parameters
Phonon Spectrum	Debye Form	θ = 295K $q_D = k_F$
Geometrical Structure Factor	Percus-Yevick Hard Sphere Form	η = 0.525 k_p = 2.6 Å^{-1}
Fermi Wavenumbers	For Zn Concentration	0.225, $2k_F$ = 2.77 Å^{-1}
	For Zn Concentration	0.35, $2k_F$ = 2.98 Å^{-1}

Table II summarizes many of the principal experimental results regarding electrical transport for $T \lesssim \theta$ in a-MgZn and also in a-AuSn and a-CuSn alloys along with corresponding theoretical results based upon Mg and Zn pseudopotentials and the adjusted phase shift matrix elements for the saturated and unsaturated cases. Generally, the adjusted phase shift matrix element in the unsaturated case yields better agreement with the detailed experimental results than the Born approximation results and the phase shift results <u>including saturation</u> yield the best agreement with experiment in the a-MgZn alloys. Furthermore, there is excellent qualitative agreement between

TABLE II. A SUMMARY OF THEORETICAL AND EXPERIMENTAL RESULTS IN LOW RESISTIVITY AMORPHOUS ALLOYS. THE "BRILLOUIN SCATTERING PART" REFERS TO THE PART OF THE RESISTIVITY ARISING FROM THE DELTA FUNCTION AT K = 0 IN a(K). THE VALUES OF $2k_F$ AND k_p AND HENCE $2k_F/k_p$ IN THE a-MgZn ALLOYS WERE EXPERIMENTALLY DETERMINED; THE VALUES OF $2k_F/k_p$ GIVEN FOR a-CuSn ARE NFE VALUES AND ARE CONSISTENT WITH THE CONCENTRATION DEPENDENCE OF ρ; THE CONCENTRATION DEPENDENCE OF ρ IN a-AuSn SUGGESTS THAT $2k_F/k_p$ IS ~ 10% LESS THAN NFE VALUES. THE COEFFICIENT A IS DEFINED BY $\rho \approx \rho_o(1+AT^2)$ FOR 5K < T < 40K. THE COEFFICIENT B IS DEFINED BY $\rho \approx \rho_1 - BT^{3/2}$ FOR T_M < T < 240K. THE COLUMN HEADED AVG LISTS AVERAGE VALUES FOR THE ALLOYS STUDIED IN REFERENCE 24.

Alloy	a-MgZn							a-CuSn		a-AuSn	
Theory/Expt	Theory				Expt			Expt		Expt	
Z	2				2			1.6	3.4	1.6	3.4
$2k_F/k_p$	1.11				Avg.	1.06	1.15	~1.0	~1.3		
Potential	Pseudo Mg	Pseudo Zn	Phase Shift								
$q_D\Lambda$	∞	∞	∞	11.7							
$\rho(\theta_D)(\mu\Omega cm)$	20	29	53	53	53	49	57	112	65	99	60
10^4 TCR$(\theta_D)(K^{-1})$	-0.13	1.2	-0.87	-1.2	-1.9	-1.5	-2.0	-1.3	0.6	-1.4	0.8
10^4 (Brillouin part)	0.32	0.33	2.7×10^{-4}								
T_M (K)	>150	None	90	46	47	55	40	Monotonic at extremes		18	43
$10^3[\rho(T_M)/\rho(0°K)-1]$			3.0	0.62	0.69	1.11	0.37				
10^4 B ($\mu\Omega cmK^{-3/2}$)				3.7	4.5	3.5	5.5				
10^6 A (K^{-2})			1.01	0.48	0.50						

the phase shift results and the amorphous noble metal based data. These results strongly suggest that saturation effects or Mooij phenomena are readily observable in amorphous alloys with resistivity as low as 50 μΩcm.

Let us now turn to a brief description of our results for the various temperature regions studied in detail by Matsuda and Mizutani[24] in a-MgZn and the overall temperature dependences predicted for the other known low resistivity amorphous alloys.

A. The room temperature ($T \approx \theta$) TCR.

The high temperature ($T \gtrsim \theta$) form for the (effective) resistivity static structure factor to first order in $\alpha(K)$ is

$$S^{\rho}(K) \cong a(K)e^{-\alpha(K)/4} + \alpha(K)(T/\theta)[A^{\rho}(K)(1-\gamma)-a(K)e^{-\alpha(K)/4}] \qquad (9)$$

where $\gamma = 0$ in the standard diffraction model (i.e. no saturation) and for Pippard or sharp cutoff saturation $\gamma \approx \rho/\rho^*$. Generally, $\rho^* \approx 200$ μΩcm in high resistivity systems[14-17] and so we have taken $\gamma \approx 1/4$ in a-MgZn. This was the basis for our choice of $q_D\Lambda = 11.7$ in Pippard saturation. The high temperature limiting form of the averaged resistivity structure factor $A^{\rho}(K)$, as defined in References 6-9 is given by

$$A^{\rho}(K) = \int_0^1 d\left(\frac{q}{q_D}\right) \int \frac{d\Omega q}{4\pi}\, a(|\vec{K}+\vec{q}|) \qquad (10)$$

The sign of the contribution to the TCR from scattering vector K is determined by $A^{\rho}(K)(1-\gamma) - a(K)e^{-\alpha(K)/4}$. In the extreme backscattering case (as is often assumed for TM based amorphous alloys) one has $\rho \propto S^{\rho}(2k_F)$ and the TCR is negative if $a(2k_F)e^{-\alpha(2kF)/4} > A^{\rho}(2k_F)(1-\gamma)$; in particular, for no saturation and Percus-Yevick structure factors with packing fraction 0.525 (appropriate for a large class of amorphous metals) negative TCR would be predicted for

$0.9 \lesssim \frac{2k_F}{k_F} \lesssim 1.1$. On the other hand, when a relatively broad range of scattering vectors yield significant contributions to ρ and the TCR, one must employ Eq. (1) to determine $\rho(T)$, and this simple criterion for the occurrence of negative TCR is invalid. Saturation effects will also invalidate this criterion; the range of $2k_F/k_p$ for negative TCR is increased when $\gamma > 0$, and negative TCR will generally occur for all $2k_F/k_p$ values when $\gamma \gtrsim 0.5$.

The computed TCR's in a-MgZn are listed in Table II for the various conditions considered. The "Brillouin scattering" contribution,[6,10] which arises from the delta function at $K = 0$ in $a(K)$ and gives the normal scattering contribution in the crystalline case, is listed separately in Table II to indicate the relative importance of this term. (We have generally assumed that Brillouin scattering contributions are negligible in TM based amorphous alloys since backscattering is expected to dominate.)

A number of interesting features are indicated:

(i) The range of $2k_F/k_p$ for which negative TCR's are predicted with the phase shift approximation in Eq. (1) is shifted toward considerably higher values than those given in the extreme backscattering case. The Mg pseudopotential results suggest a similar but smaller shift. The range of $2k_F/k_p$ for negative TCR in saturated and unsaturated cases (excluding the Zn pseudopotential case) are consistent with the data of Reference 24. Negative TCR values were obtained for $0.96 \lesssim 2k_F/k_p \lesssim 1.24$ in the unsaturated case; the range, when saturation effects ($q_D\Lambda = 11.7$) are included is $0.94 \lesssim 2k_F/k_p \lesssim 1.29$.

(ii) The computed Brillouin scattering contribution to the TCR is negligible in the phase shift formulation, but is significant in the Born approximation case. For the Zn pseudopotential, negative TCR's are completely eliminated by the Brillouin contribution. Frobose and Jackle[10] had encountered similar difficulties with their Born approximation calculations on a-CuSn.

(iii) The Born approximation results for the TCR are in poor agreement with experiment. The phase shift results are about half as large as the observed TCR.

B. The low temperature T^2 region, minima, and maxima in $\rho(T)$.

The low temperature limiting form of the resistivity static structure factor,[6-9] neglecting saturation is

$$S\rho(K) = a(K) + (\pi^2/6)\ a(K)\alpha(K)(T/\theta)^2 \qquad (11)$$

Thus, the standard diffraction model yields a positive quadratic temperature dependence for the resistivity near 0°K, independent of the sign of the TCR at high temperatures. Consequently, a general feature of the standard diffraction model is that if the room temperature TCR is negative, the resistivity will exhibit small maxima in $\rho(T)$. (This simple result is often ignored, leading to improper conclusions regarding agreement between theory and experiment in high resistivity amorphous alloys.) Matsuda and Mizutani[24] observe a quadratic $\rho(T)$ in a-MgZn below 30K, which they attribute to the low temperature form of the theory based upon Eqs. (1) and (11). However, detailed calculations indicate that significant deviations from Eq. (11) occur above about 5K for K near k_p so this interpretation is questionable; in particular, the low temperature limit of the T^2 coefficient will generally not

be observed above ~ 5K. Nevertheless, the standard diffraction model results for a-MgZn are consistent with a quadratic $\rho(T)$ in the range from 5 to 30K. However, the computed coefficient of the quadratic term, given in Table II, is smaller than the low temperature limit (which is about $2\times10^{-6}K^{-2}$) in the unsaturated case but is still larger than the measured coefficient by a factor of two. When saturation is included, excellent agreement with the measured coefficient is obtained.

Figure 2 shows the ρ vs. T curves obtained by Matsuda and Mizutani[24] for a-MgZn alloys between 2 and 70K. Small maxima in the resistivity ($\rho(T_M) - \rho(0°K) \approx 10^{-3}\ \rho(0°K)$) are observed for $T_M \approx 50K$ where T_M is the temperature at the resistivity maxima. Figure 3(a) shows phase shift based standard diffraction model results. The $2k_F/k_p = 1.1$ case is appropriate for a-MgZn and is in qualitative agreement with the experimental results shown in Figure 2. However, the computed maximum occurs at $T_M \approx 0.3\ \theta$, which corresponds to $T_M \approx 90K$ and the computed maximum is substantially larger than observed. When saturation is included, excellent agreement (see Table II and Figure 3(b)) in the position and size of the maximum is obtained. The Born approximation results at these temperatures are in very poor agreement with experiment.

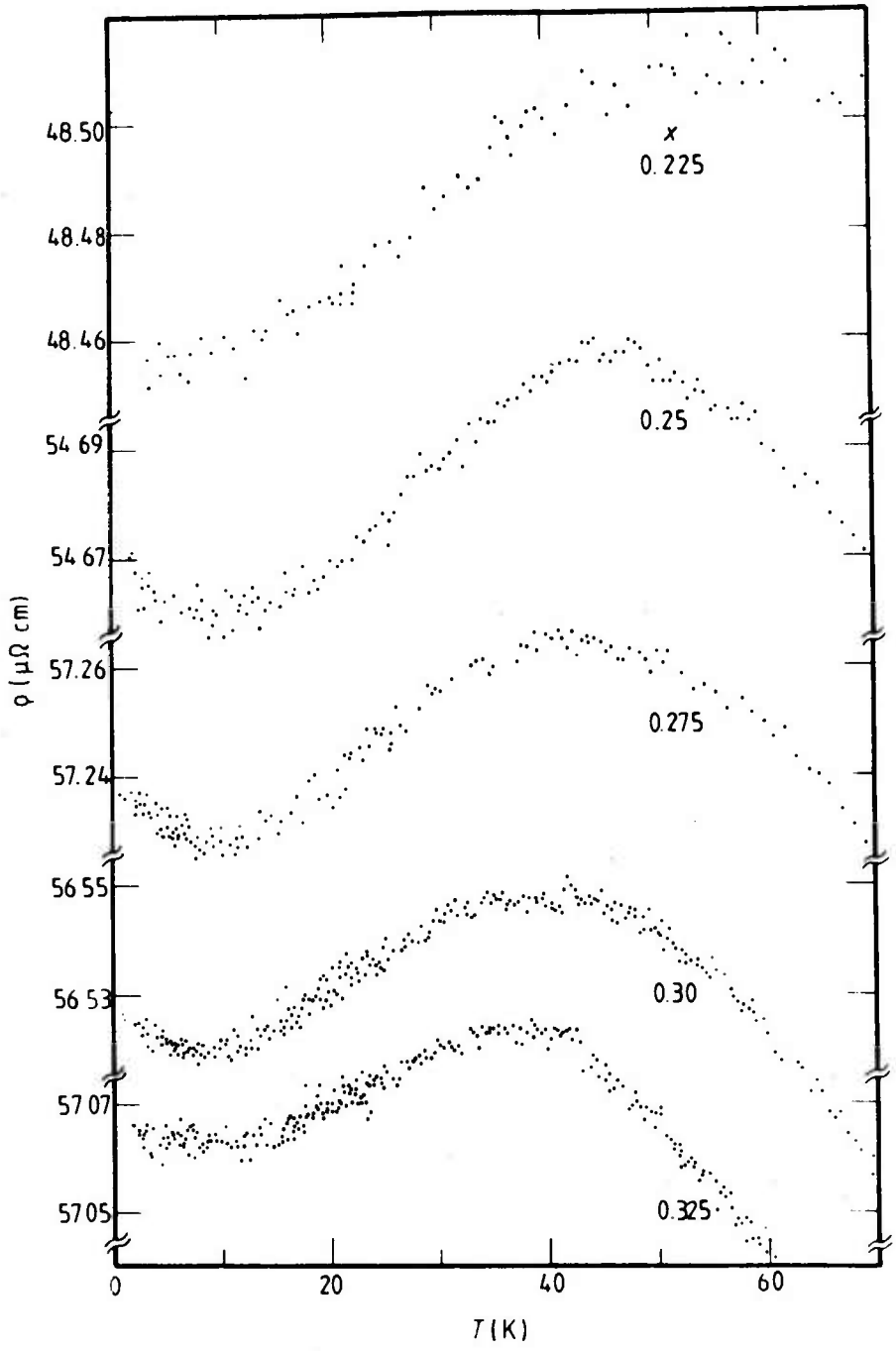

Figure 2. Electrical Resistivity vs. Temperature below 70K in a—^{Mgzn} from Ref. 24.

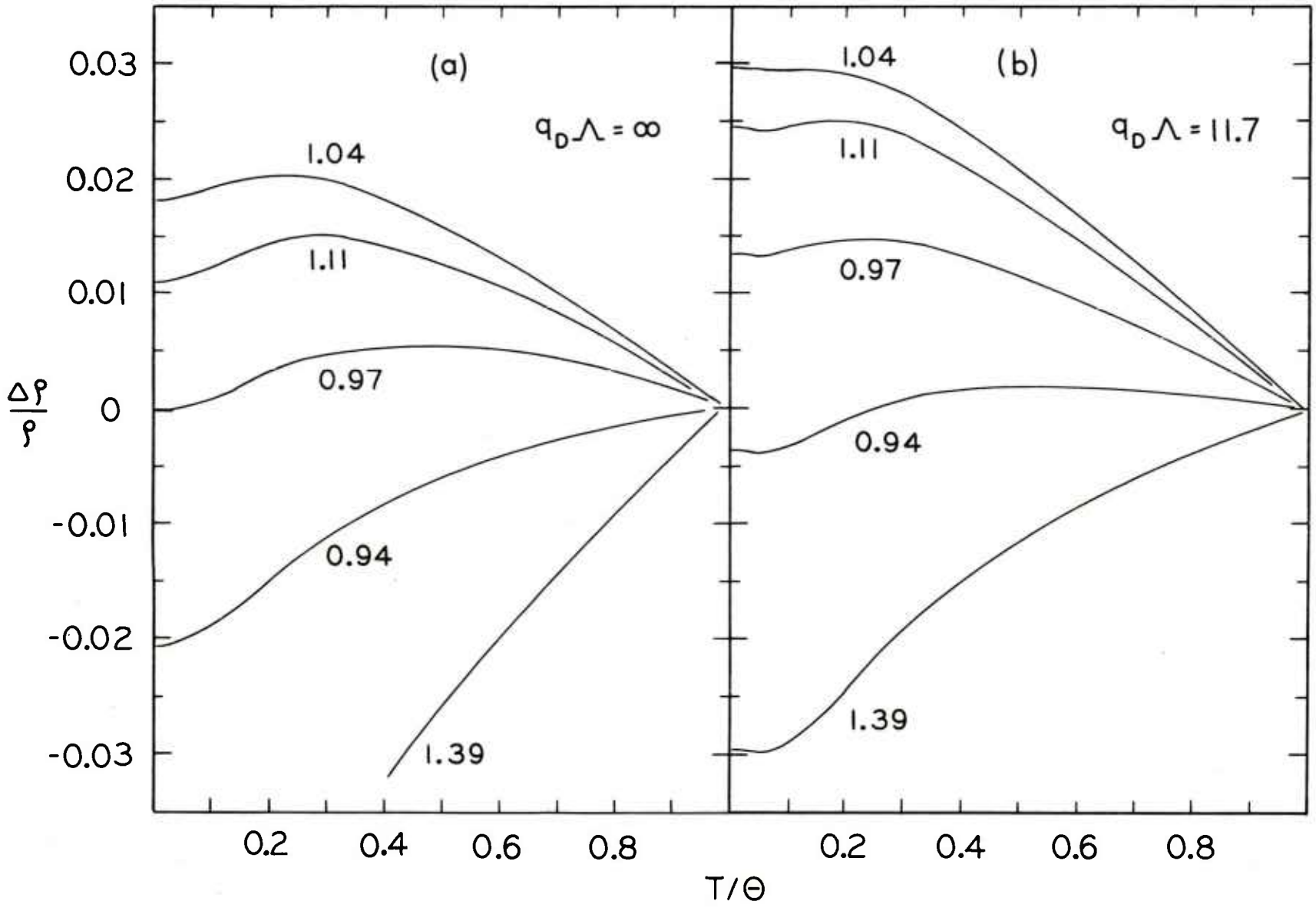

Figure 3. The relative change in the resistivity vs. T/Θ computed from the diffraction model with the adjusted phase shift expanded potential appropriate to a-MgZn.

The data of Figure 2 exhibit another interesting feature, viz. small minima at about 10K. This feature is not consistent with standard diffraction model predictions. However, as may be seen in Figure 3(b) or from the results listed in Table II, the theory including saturation is again in excellent agreement with the data. This is a particularly interesting result since to observe such effects, $q_D\Lambda$ has to be large enough to produce an observable minimum but not so large as to produce monatonic decreasing $\rho(T)$; also the alloys under investigation must be free of effects associated with magnetic ions or transitions to superconductivity. (Essentially the same results, although with deeper minima, are obtained in the case of sharp cutoff saturation corresponding to $\gamma = 1/4$.) It is possible, of course, that this agreement is fortuitous.

C. Other low resistivity amorphous alloys.

Other low resistivity ($\rho < 100$ $\mu\Omega$cm) amorphous alloys with $2k_F/k_p \gtrsim 1$ that we are aware of and for which the temperature dependence of the electrical resistivity has been determined, are a-CuSn,[22] a-AuSn,[23] a-AuIn,[23] a-MgCu,[25], a-AgCuAl,[26] a-AgCuMg,[26] and a-AgCuGe.[26] These alloys have been studied over wide ranges of temperature and composition which correspond to extensive ranges in $2k_F/k_p$; for example, for a-CuSn and a-AuSn, this range varies from about 1.0 to about 1.3. Figure 3 shows theoretical results for similar ranges in $2k_F/k_p$ in the saturated and unsaturated cases and parameters appropriate to the a-MgZn alloys.

Before the results exhibited in Figure 3 are compared with measurements in the other alloys, we make the following comments: (i) The magnitude of the

variations in the electrical resistivity with T in the range from 0°K to θ is governed essentially by $M\theta$. Hence, although the effective masses are larger, the expected lower Debye temperatures for these noble metal based alloys relative to a-MgZn, can account for the fact that the temperature dependent effects in the resistivity are of the same magnitude. (ii) The range of resistivities in the other alloys is considerably larger than in the a-MgZn alloys. Thus, we cannot expect $q_D\Lambda = 11.7$ to be appropriate for all these alloys. This effect can be significant; e.g., for $\rho \approx 100$ $\mu\Omega$cm, saturation effects could completely eliminate the small maximum in $\rho(T)$, for $2k_F \approx k_p$, yielding a monotonic decreasing function. (In fact, this was observed in Reference 23 for the a-AuSn alloy with $\rho \approx 100$ $\mu\Omega$cm.) (iii) There could be appreciable short range order effects produced by the differences in effective potential and application of the "substitutional model" might not be appropriate for such different ionic constituents as occur in these alloys.

In spite of these difficulties, all the low resistivity alloy systems exhibit the general features shown in Figure 3 including resistivity maxima in negative TCR cases. This strongly suggests that matrix elements of the form given in the phase shift expansion rather than Born approximation pseudopotential is appropriate in these alloys. The temperature dependences of the various composition (i.e., various $2k_F/k_p$) a-CuSn alloys are in remarkable agreement with the saturated case curves in Figure 3(b) if we use free electron theory to compute $2k_F/k_p$ for each composition. Similar consistency is obtained for the a-AuSn data if we deduce $2k_F/k_p$ from the ρ and TCR vs. composition data shown in Reference 23 (which leads to $2k_F$ values about 10 percent

smaller than free electron values). The a-MgCu[25] data are essentially identical to those of a-MgZn. The AgCu based alloys[26] offer a particularly clear illustration of the shift to higher values for the $2k_F/k_p$ range of negative TCR values.

D. The $(T-T_M)^{3/2}$ temperature dependence.

Matsuda and Mizutani[24,25] discovered that over an extensive range of temperature to the right of T_M, the resistivity in the a-MgZn and a-MgCu alloys has the form

$$\rho(T) = \rho_1 - B(T-T_M)^{3/2} \qquad (12)$$

The phase shift calculation, including saturation, fits this equation, and thus the experimental data, surprisingly well both with regard to the value of B (Table II) and the linearity of the ρ vs. $(T-T_M)^{3/2}$ as seen in Figure 4.

SUMMARY AND CONCLUSIONS

Electrical resistivity of low resistivity ($\rho < 100$ $\mu\Omega$cm) amorphous metals has been studied in the context of the Ziman-Faber diffraction model which has been generalized to account for saturation effects by incorporation of the "Pippard function"[20] which describes the reduction of the electron-phonon interaction at small $q\Lambda$ where q is the phonon wave number and Λ the electron mean free path. The standard diffraction model formulae are obtained in the limit that Λ goes to infinity. (Essentially equivalent results were obtained using a "sharp cutoff" form to describe saturation effects.)

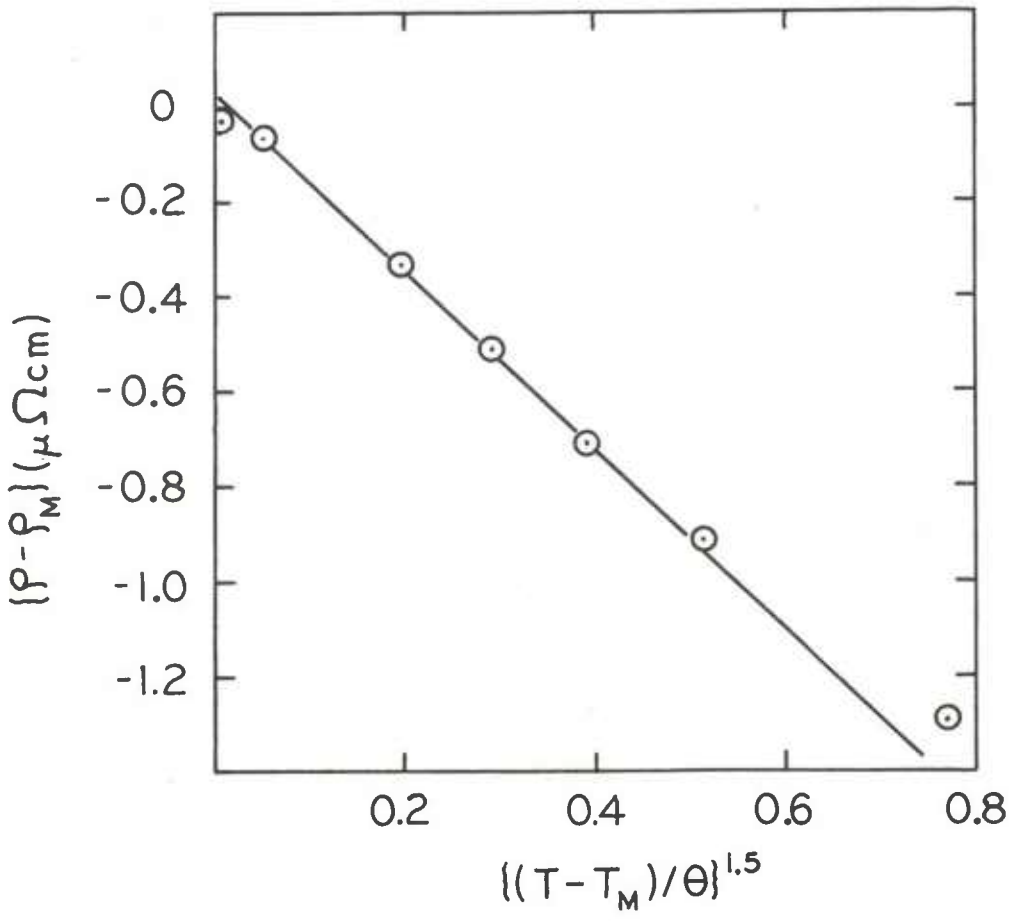

Figure 4. the 3/2 power region to the right of the resistivity maximum in a—MgZn

The specific computational results were obtained for a-MgZn alloys which comprise an ideal system to test the diffraction model because of their relatively simple electronic structure, low resistivity, and the existence of detailed experimental data covering temperatures from 2 to 300K in a series of well characterized alloys. Moreover, the similarity of the atomic structures and ionic radii of Mg and Zn allow us to make the further computational simplification of adopting the Faber-Ziman substitutional model.[5] The parameters used in the computations and listed in Table I are thus appropriate to the a-MgZn alloys.

Pseudopotential matrix elements in the Born approximation and an adjusted phase shift scattering matrix element were employed. The phase shift expanded form was assumed to include only s and p components (from consideration of the atomic structure of Mg and Zn) and the phase shifts were adjusted to yield the observed magnitude of ρ and to satisfy the Friedel sum rule. The Mg and Zn pseudopotentials were taken from Harrison.[28] These two types of matrix elements are quite different in form. The cancellation near $2k_F$, characteristic of pseudopotentials, does not appear in the adjusted phase shift expanded matrix element.

The adjusted phase shift results, neglecting saturation ($\Lambda \to \infty$), are in qualitative agreement with the data, exhibiting all the observed features of the experimental data in a-MgZn except for the small minimum at about 5K. The phase shift results, including saturation with $q_D\Lambda = 11.7$ (chosen in accordance with the ideas presented in Reference 17), are in remarkable agreement with the observed details of the temperature dependence of the electrical resistivity in the a-MgZn alloys.[24] This includes the room temperature TCR, the shape and extent of the $(T-T_M)^{3/2}$ region to the right of the maximum, the magnitude and position of the maximum, the shape and extent of the quadratic in T region, and even the position and size of the minimum near 5K.

We also note that negative TCR's occur at significantly higher $2k_F/k_p$ values than predicted with the extreme backscattering approximation and are consistent with the data of References 24-26. Furthermore, the adjusted phase shift results, including saturation, and with appropriate values of $2k_F/k_p$, are in good qualitative agreement with $\rho(T)$ in the other low resistivity amorphous alloys[22,23,25,26] which have been studied. On the other hand, although the Born approximation results are within a factor of two of the observed magnitude of ρ, they fail to exhibit the temperature dependence of ρ observed in the low resistivity amorphous alloys.

The following conclusions may be drawn from the above results:

(a) The diffraction model, with appropriate matrix elements and incorporated phonon ineffectiveness effects at small $q\Lambda$, can explain the observed temperature dependence of ρ in low resistivity ($\rho < 100$ $\mu\Omega$cm) amorphous alloys. Qualitative agreement with experiment is obtained if

saturation effects are neglected. This latter is to be contrasted with the situation in high resistivity amorphous metals, where not even qualitative agreement with the observed temperature dependence of ρ can be obtained if saturation effects are not included in the diffraction model.

(b) Saturation or Mooij effects are important even for resistivities as low as 50 $\mu\Omega$cm. Moreover, the reduction in electron-phonon interaction (phonon ineffectiveness) can be adequately represented by the classically derived Pippard function[20] or even a "sharp cutoff" form. Apparently a consistent procedure based upon a generalization of the diffraction model, which assumes that saturation effects in elastic scattering are negligible, describes the temperature dependence of the resistivity equally well for alloys whose resistivity is 50 $\mu\Omega$cm or 150 $\mu\Omega$cm. This is particularly remarkable because it seems obvious that localization effects must eventually lead to a failure of this simple scattering picture and 150 $\mu\Omega$cm corresponds to Λ of the order of interatomic spacings.

(c) There is strong evidence that the Born approximation is not appropriate for studies of the temperature dependence of ρ in many disordered metals. Support for this is found in the studies of ρ in a-CuSn by Frobose and Jackle,[10] the investigation of monovalent liquid metals by Young, Meyer, and Kilby,[36] the study of liquid Ca, Sr, and Ba by Ratti and Evans,[38] in addition to the present results.

REFERENCES

1. J. M. Ziman, Electrons and Phonons, Clarendon Press, Oxford, (1960).
2. T. E. Faber, An Introduction to the Theory of Liquid Metals, Cambridge University Press, London, (1972).
3. G. Baym, Phys. Rev. 135, A1691 (1964).
4. L. van Hove, Phys. Rev. 95, 294 (1954).
5. T. E. Faber and J. M. Ziman, Phil. Mag. 11, 153 (1965).
6. P. J. Cote and L. V. Meisel, Glassy Metals I, Ed. H.-J. Guntherodt and H. Beck, Springer, Heidelberg, pp. 141-166 (1981).
7. P. J. Cote and L. V. Meisel, Phys. Rev. Lett. 39, 102 (1977).
8. L. V. Meisel and P. J. Cote, Phys. Rev. B 16, 2978 (1977).
9. L. V. Meisel and P. J. Cote, Phys. Rev. B 17, 4652 (1978).
10. K. Frobose and J. Jackle, J. Phys. F 7, 2331 (1977).
11. S. R. Nagle, Phys. Rev. B 16, 1694 (1977).
12. See, for example, Reference 1, Chapter IX.
13. J. H. Mooij, Phys. Status Solidi A 17, 521 (1973).
14. Z. Fisk and G. W. Webb, Phys. Rev. Lett. 36, 1084 (1976).
15. F. J. Ohkawa, Tech. Rept. Inst. Solid State Physics A 842 (1977).
16. N. Morton, B. W. James, and G. H. Westenholm, Cryogenics, 131 (1978).
17. P. J. Cote and L. V. Meisel, Phys. Rev. Letters 40, 1586 (1978).
18. E.g., G. Bergmann and P. Marquardt, Phys. Rev. B 18, 326 (1978), Y. Waseda and H. S. Chen, Phys. Status Solidi (b) 87, 777 (1978), or L. V. Meisel and P. J. Cote, Phys. Rev. B 15, 2970 (1977).
19. E.g., P. B. Allen and B. Chakraborty, Phys. Rev. B 23, 4815 (1981).

20. A. B. Pippard, Phil. Mag. 46, 1104 (1955). See also Chapter V of Reference 1 and W. A. Fate, Ph.D. Thesis, Rensselaer Polytechnic Institute, 1967, unpublished.

21. E.g., M. Jonson and S. M. Girvin, Phys. Rev. Lett. 43, 1447 (1979) or Y. Imry, Phys. Rev. Lett. 44, 469 (1980), or W. L. McMillan, Phys. Rev. B 24, 2739 (1981).

22. D. Korn, W. Murer, and G. Zibold, Phys. Lett., 47 A, 117 (1972).

23. E. Blasberg, D. Korn, H. Pfeifle, J. Phys. F 9, 1821 (1979).

24. T. Matsuda and U. Mizutani, Proc. of Fourth International Conference on Rapidly Quenched Metals, Sendai, Japan, 1981; J. Phys. F. 12, 1877 (1982). Similar but less detailed resistivity results can be found in M. N. Baibich, W. B. Muir, Z. Altounian, and Tu Guo-Hua, Phys. Rev. B 26, 2963 (1982).

25. T. Matsuda and U. Mizutani, Solid State Comm. 44, 145 (1982).

26. U. Mizutani and T. Yoshida, J. Phys. F. 12, 2331 (1982).

27. J. Hafner, E. Gratz, and H.-J. Guntherodt, Journal de Physique, 41, C8-512 (1980).

28. W. A. Harrison, Pseudopotentials in the Theory of Metals, Benjamin, New York, 1966, p. 309ff. The pseudopotentials were calculated by A. E. O. Animalu based upon the method of V. Heine and I. V. Aberenkov, Phil. Mag., 9, 451 (1964).

29. R. Evans, B. L. Gyorffy, N. Szabo, J. M. Ziman, Properties of Liquid Metals, ed. by S. Takeushi, Wiley, New York, 1973. See also R. Evans, D. A. Greenwood, and P. Lloyd, Phys. Lett. A 35, 57 (1971).

30. E.g., L. J. Sham and J. M. Ziman, Solid State Physics, Vol. 15, ed. by F. Seitz and D. Turnbull, Academic Press, New York (1963) or I. Hernandez-Calderone, J. S. Helman, and H. Vucetich, Phys. Rev. B 14, 2310 (1976).

31. J. K. Percus and G. J. Yevick, Phys. Rev. 110, 1 (1957); see also J. L. Lebowitz, ibid, 133, A1399 (1964).

32. L. von Heimendahl, J. Phys. F9, 161 (1979).

33. J. M. Ziman, Electrons and Phonons, Clarendon Press, Oxford, (1960), p. 227.

34. A. E. Dunsworth, Phys. Rev. B 12, 2030 (1975).

35. See, for example, M. J. G. Lee and V. Heine, Phys. Rev. B 5, 2829 (1972) and the discussion in Reference 34.

36. W. H. Young, Axel Meyer, and G. E. Kilby, Phys. Rev. 160, 160 (1967).

37. See, for example, Reference 2, Table 5.2 or N. W. Ashcroft and J. Leckner, Phys. Rev. 145, 83 (1966).

38. V. K. Ratti and R. Evans, J. Phys. F 13, L738 (1973).

39. T. Mizoguchi, N. Shiotani, U. Mizutani, T. Kudo, and S. Yamada, J. de Physique, 41, C8-183 (1980).

40. U. Mizutani and T. Mizoguchi, J. Phys. F 11, 1385 (1981).

TECHNICAL REPORT INTERNAL DISTRIBUTION LIST

	NO. OF COPIES
CHIEF, DEVELOPMENT ENGINEERING BRANCH	
ATTN: DRSMC-LCB-D	1
-DP	1
-DR	1
-DS (SYSTEMS)	1
-DS (ICAS GROUP)	1
-DC	1
CHIEF, ENGINEERING SUPPORT BRANCH	
ATTN: DRSMC-LCB-S	1
-SE	1
CHIEF, RESEARCH BRANCH	
ATTN: DRSMC-LCB-R	2
-R (ELLEN FOGARTY)	1
-RA	1
-RM	1
-RP	1
-RT	1
TECHNICAL LIBRARY ATTN: DRSMC-LCB-TL	5
TECHNICAL PUBLICATIONS & EDITING UNIT ATTN: DRSMC-LCB-TL	2
DIRECTOR, OPERATIONS DIRECTORATE	1
DIRECTOR, PROCUREMENT DIRECTORATE	1
DIRECTOR, PRODUCT ASSURANCE DIRECTORATE	1

NOTE: PLEASE NOTIFY DIRECTOR, BENET WEAPONS LABORATORY, ATTN: DRSMC-LCB-TL, OF ANY ADDRESS CHANGES.

TECHNICAL REPORT EXTERNAL DISTRIBUTION LIST

	NO. OF COPIES
ASST SEC OF THE ARMY RESEARCH & DEVELOPMENT ATTN: DEP FOR SCI & TECH THE PENTAGON WASHINGTON, D.C. 20315	1
COMMANDER DEFENSE TECHNICAL INFO CENTER ATTN: DTIC-DDA CAMERON STATION ALEXANDRIA, VA 22314	12
COMMANDER US ARMY MAT DEV & READ COMD ATTN: DRCDE-SG 5001 EISENHOWER AVE ALEXANDRIA, VA 22333	1
COMMANDER ARMAMENT RES & DEV CTR US ARMY AMCCOM ATTN: DRSMC-LC(D)	1
DRSMC-LCE(D)	1
DRSMC-LCM(D) (BLDG 321)	1
DRSMC-LCS(D)	1
DRSMC-LCU(D)	1
DRSMC-LCW(D)	1
DRSMC-SCM-O (PLASTICS TECH EVAL CTR, BLDG. 351N)	1
DRSMC-TSS(D) (STINFO) DOVER, NJ 07801	2
DIRECTOR BALLISTICS RESEARCH LABORATORY ARMAMENT RESEARCH & DEV CTR US ARMY AMCCOM ATTN: DRSMC-TSB-S (STINFO) ABERDEEN PROVING GROUND, MD 21005	1
MATERIEL SYSTEMS ANALYSIS ACTV ATTN: DRSXY-MP ABERDEEN PROVING GROUND, MD 21005	1
COMMANDER US ARMY AMCCOM ATTN: DRSMC-LEP-L(R) ROCK ISLAND, IL 61299	1
COMMANDER ROCK ISLAND ARSENAL ATTN: SMCRI-ENM (MAT SCI DIV) ROCK ISLAND, IL 61299	1
DIRECTOR US ARMY INDUSTRIAL BASE ENG ACTV ATTN: DRXIB-M ROCK ISLAND, IL 61299	1
COMMANDER US ARMY TANK-AUTMV R&D COMD ATTN: TECH LIB - DRSTA-TSL WARREN, MI 48090	1
COMMANDER US ARMY TANK-AUTMV COMD ATTN: DRSTA-RC WARREN, MI 48090	1
COMMANDER US MILITARY ACADEMY ATTN: CHMN, MECH ENGR DEPT WEST POINT, NY 10996	1
US ARMY MISSILE COMD REDSTONE SCIENTIFIC INFO CTR ATTN: DOCUMENTS SECT, BLDG. 4484 REDSTONE ARSENAL, AL 35898	2
COMMANDER US ARMY FGN SCIENCE & TECH CTR ATTN: DRXST-SD 220 7TH STREET, N.E. CHARLOTTESVILLE, VA 22901	1

NOTE: PLEASE NOTIFY COMMANDER, ARMAMENT RESEARCH AND DEVELOPMENT CENTER, US ARMY AMCCOM, ATTN: BENET WEAPONS LABORATORY, DRSMC-LCB-TL, WATERVLIET, NY 12189, OF ANY ADDRESS CHANGES.

TECHNICAL REPORT EXTERNAL DISTRIBUTION LIST (CONT'D)

	NO. OF COPIES
COMMANDER US ARMY MATERIALS & MECHANICS RESEARCH CENTER ATTN: TECH LIB - DRXMR-PL WATERTOWN, MA 01272	2
COMMANDER US ARMY RESEARCH OFFICE ATTN: CHIEF, IPO P.O. BOX 12211 RESEARCH TRIANGLE PARK, NC 27709	1
COMMANDER US ARMY HARRY DIAMOND LAB ATTN: TECH LIB 2800 POWDER MILL ROAD ADELPHIA, MD 20783	1
COMMANDER NAVAL SURFACE WEAPONS CTR ATTN: TECHNICAL LIBRARY CODE X212 DAHLGREN, VA 22448	1
DIRECTOR US NAVAL RESEARCH LAB ATTN: DIR, MECH DIV CODE 26-27, (DOC LIB) WASHINGTON, D.C. 20375	1 1
COMMANDER AIR FORCE ARMAMENT LABORATORY ATTN: AFATL/DLJ AFATL/DLJG EGLIN AFB, FL 32542	1 1
METALS & CERAMICS INFO CTR BATTELLE COLUMBUS LAB 505 KING AVENUE COLUMBUS, OH 43201	1

NOTE: PLEASE NOTIFY COMMANDER, ARMAMENT RESEARCH AND DEVELOPMENT CENTER, US ARMY AMCCOM, ATTN: BENET WEAPONS LABORATORY, DRSMC-LCB-TL, WATERVLIET, NY 12189, OF ANY ADDRESS CHANGES.

READER EVALUATION

Please take a few minutes to complete the questionnaire below and return to us at the following address: Commander, Armament Research and Development Center, U.S. Army AMCCOM, ATTN: Technical Publications, DRSMC-LCB-TL, Watervliet, NY 12189.

1. Benet Weapons Lab. Report Number _____

2. Please evaluate this publication (check off one or more as applicable).

	Yes	No
Information Relevant	_____	_____
Information Technically Satisfactory	_____	_____
Format Easy to Use	_____	_____
Overall, Useful to My Work	_____	_____

Other Comments _____

_____

_____

3. Has the report helped you in your own areas of interest? (i.e. preventing duplication of effort in the same or related fields, savings of time, or money). _____

_____

_____

4. How is the report being used? (Source of ideas for new or improved designs. Latest information on current state of the art, etc.). _____

_____

_____

5. How do you think this type of report could be changed or revised to improve readability, usability? _____

_____

_____

6. Would you like to communicate directly with the author of the report regarding subject matter or topics not covered in the report? If so please fill in the following information.

Name: _____

Telephone Number: _____

Organization Address: _____

_____